JOURNAL OF APPLIED ELECTROCHEMISTRY 19 (1989) 630–636

Electrode current distribution in a hypochlorite cell*

L. R. CZARNETZKI, L. J. J. JANSSEN

Department of Chemical Technology, Eindhoven University of Technology, 5600 MB Eindhoven, The Netherlands

Received 12 July 1988; revised 5 January 1989

Electrochemical production of gases, e.g. Cl_2, H_2 and O_2, is generally carried out in vertical electrolysers with a narrow electrode gap. The evolution of gas bubbles, on one hand, speeds up the mass transport; on the other it increases the solution resistance and also the cell potential. The gas void fraction in the cell increases with increasing height and, consequently, the current density is expected to decrease with increasing height. Insight into the effects of various parameters on the current distribution and the ohmic resistance in the cell is of the utmost importance in understanding the electrochemical processes at gas-evolving electrodes. An example of the described phenomena is the on-site production of hypochlorite by means of a vertical cell. Experiments were carried out with a working electrode consisting of 20 equal segments and an undivided counter electrode. It has been found that the current distribution over the anode is affected by various electrolysis parameters. The current density, j, decreased linearly with increasing distance, h, from the leading edge of the electode. The absolute value of the slope of the I/h straight line increased with increasing average current density and temperature, and with decreasing velocity of the solution, NaCl concentration and interelectrode gap.

Nomenclature

a_1	constant
b_a	anodic Tafel slope (V)
b_c	cathodic Tafel slope (V)
B	current distribution factor
B_0	current distribution factor at $t_e = 0$
c_{NaCl}	sodium chloride concentration (kmol m^{-3})
d_{wt}	interelectrode gap (mm)
h	distance from the leading edge of the segmented electrode (m)
H	total height of the segmented electrode (m)
I	current (A)
I_s	current through a segment (A)
j_0	exchange current density (kA m^{-2})
j_{av}	mean current density (kA m^{-2})
j_t	current density at the top of the segmented electrode ($h = H$) (kA m^{-2})
j_b	current density at the bottom of the segmented electrode ($h = 0$) (kA m^{-2})
n_s	number of a segment of the segmented electrode from its leading edge
R_s	unit surface resistance of solution (Ω m^2)
$R_{s,b}$	unit surface resistance of solution at the bottom of the segmented electrode (Ω m^2)
$R_{s,t}$	unit surface resistance of solution at the top of the segmented electrode (Ω m^2)
t_e	time of electrolysis (h)
T	temperature (K)
U_c	cell voltage (V)
U_0	reversible cell voltage (V)
v_0	solution flow rate of the bulk solution in the cell at the level of the leading edge of the electrode (m s^{-1})
ϱ	resistivity of the solution (Ω m)
η_a	anodic overpotential (V)
η_c	cathodic overpotential (V)
ε	gas void fraction
ε_b	gas void fraction at $h = 0$
ε_t	gas void fraction at $h = H$

1. Introduction

On-site production of hypochlorite has become more important during the last decade. It is very easy to produce hypochlorite from chlorine bubbling through an alkaline solution; however, the storage and transport of chlorine cause a large number of problems. On-site production of hypochlorite is therefore an acceptable solution, especially for developing countries. Hypochlorite is used as a purifying agent for drinking and waste water.

The most important reactions in an undivided cell for hypochlorite production are [1]:

at the anode

$$2Cl^- \longrightarrow 2e^- + Cl_2 \quad (1)$$

$$2H_2O \longrightarrow O_2 + 4H^+ + 4e^- \quad (2)$$

$$6ClO^- + 3H_2O \longrightarrow 2ClO_3^- + 4Cl^- + 3/2O_2 + 6H^+ + 6e^- \quad (3)$$

* Paper presented at the 2nd International Symposium on Electrolytic Bubbles organized jointly by the Electrochemical Technology Group of the Society of Chemical Industry and the Electrochemistry Group of the Royal Society of Chemistry and held at Imperial College, London, 31st May and 1st June 1988.

0021-891X/89 $03.00 + .12

in the solution

$$Cl_2 + H_2O \longrightarrow HClO + H^+ + Cl^- \quad (4)$$

$$HClO \rightleftharpoons ClO^- + H^+ \quad (5)$$

$$2HClO + ClO^- \longrightarrow ClO_3^- + 2Cl^- + 2H^+ \quad (6)$$

and at the cathode

$$2H_2O + 2e^- \longrightarrow H_2 + 2OH^- \quad (7)$$

$$ClO^- + H_2O + 2e^- \longrightarrow Cl^- + 2OH^- \quad (8)$$

Chlorine is formed at the anode according to Equation 1 and dissolves into the solution. Chlorine molecules react with OH^- ions, forming hypochlorite and chloride ions by Equation 4. The equilibrium concentration of Cl_2 depends on the pH. At a pH of 7 chlorine is almost completely converted to hypochlorous acid and hypochlorite ions [2].

Two side reactions occur at the anode: the formation of oxygen by the water oxidation Equation 2 and the formation of chlorate and oxygen by the oxidation of hypochlorite (Equation 3). To diminish the evolution of chlorine bubbles at the anode, to prevent the loss of chlorine gas from the electrolysis cell and to maintain a low rate of oxygen evolution, electrolyses were carried out at a pH between 9 and 12.

Hydrogen gas bubbles are evolved at the cathode according to Equation 5 and, in an undivided cell, hypochlorite is reduced by Reaction 8 [3, 4], which can be minimized by addition of sodium dichromate [5, 6].

An increase in resistance of the solution between anode and cathode is caused by the presence of gas bubbles, particularly near the electrode surfaces. This extra increase in resistance of the solution affects the current distribution over both electrodes [7]. In this paper, the current density distribution over one electrode is determined as a function of the average current density, the flow rate of the solution, the interelectrode gap, the temperature, the pH, the sodium chloride concentration and the sodium dichromate concentration.

2. Experimental details

2.1. *Electrolytic cell and electrodes*

The solution circuit consisted of a reservoir of 8000 cm^3, a pump (Schmitt, type MP 80), a thermostat (Colora, type Ultra Thermostat), a flowmeter (Fischer & Porter) and an undivided cell (Fig. 1). The height of the Perspex cell was 0.7 m from the inlet at the bottom to the outlet at the top. The working and the counter electrodes were placed in the cell against the two back walls half-way between outlet and inlet (Fig. 2). The distance between the two electrodes was varied from 2 to 7 mm by placing Perspex frames of various thicknesses between the two back walls of the cell and by sealing them with silicone rubbers of 0.5 mm thickness at each back wall. The flat working electrode, 0.50 m in height, was divided into 20 segments, each 0.020 m in width and 0.024 m in height, with a space of 1 mm between every two segments. The counter electrode was a flat plate 0.02 m in width and 0.50 m in height.

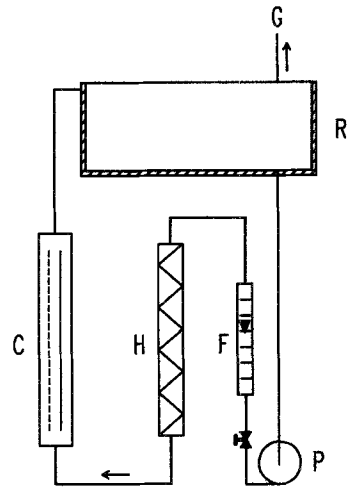

Fig. 1. Experimental set-up for the measurement of the current density distribution over the working electrode. C, electrolysis cell; H, heat exchanger; F, flow meter; P, pump; R, reservoir; G, gas outlet.

Three different combinations of flat electrodes were applied in the experiments: (1) a segmented Ti/RuO_2–TiO_2 anode combined with a one-plate titanium cathode; (2) a segmented Ti/RuO_2 anode combined with a one-plate Ti/Pt–Ir cathode; and (3) a segmented stainless steel (316 Ti) cathode combined with a one-plate Ti/Pt–Ir anode.

2.2. *Measurement of current distribution*

The potential difference between each segment of the working electrode and the counter electrode was adjusted by a special constant voltage source with 20 independent channels. Each segment was connected to the constant voltage source by two contacts, one for the power supply and the other for the control of the potential. The counter electrode had five connections for the current supply to obtain a uniform potential distribution over its whole area, and one connection for the control of the potential.

The potential range of the constant voltage source could be varied between 0 and 5 V. The maximum current output was about 100 A. In the experiments the current of each segment was subsequently measured by a.d. converters connected to a microcomputer. In order to minimize random errors, the segments were

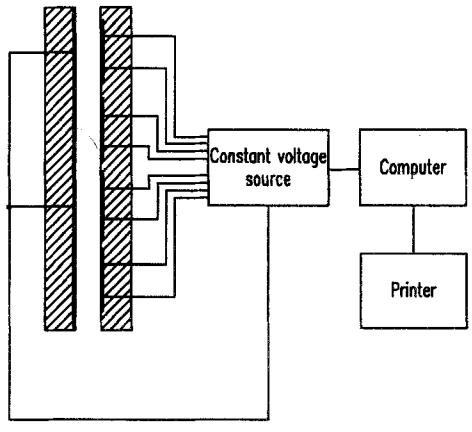

Fig. 2. Schematic plot of the electric circuit with a part of the electrolysis cell.

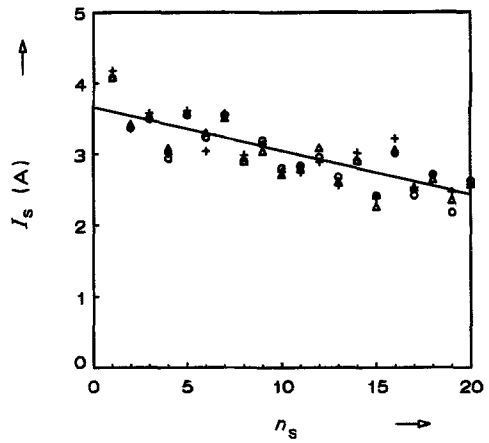

Fig. 3. The segment current, I_s, is plotted versus the segment number, n_s, for an electrolysis with a segmented Ti/RuO_2–TiO_2 anode and a one-plate titanium cathode. The electrolysis parameters are $j_{av} = 6\,kA\,m^{-2}$, $v_0 = 0.3\,m\,s^{-1}$, $T = 343\,K$, $d_{wt} = 2\,mm$, $c_{NaCl} = 1.5\,kmol\,m^{-3}$ and pH 9 (three single measurements).

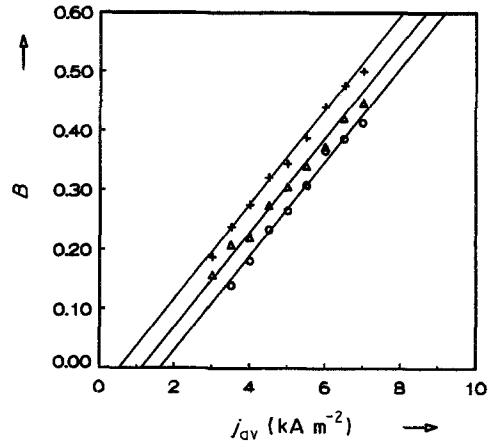

Fig. 4. B vs j_{av} curves for a segmented Ti/RuO_2–TiO_2 anode and a one-plate titanium cathode after different times of electrolysis, at $T = 343\,K$, $d_{wt} = 2\,mm$, $c_{NaCl} = 1.5\,kmol\,m^{-3}$, pH 9 and $v_0 = 0.3\,m\,s^{-1}$. (+) Curve 1, $t_e = 30\,min$; (△) curve 2, $t_e = 75\,min$; (○) curve 3, $t_e = 120\,min$.

scanned up to 50 times within 15 s. From these 50 values the average current of one segment was calculated by the computer. This procedure is considered as a single measurement. The computer was also used to store the potential between the working and the counter electrode. The current density distribution varies because of fluctuations in the behaviour of the gas–liquid mixture. This incidental error was minimized by repeating the measurements of the current density distribution several times, usually within 2 min.

2.3. *Electrolysis conditions*

The experiments were carried out with average current densities between 2 and 7 kA m^{-2} and with solution temperatures between 298 and 343 K. The concentration of the sodium chloride solution was varied betwen 1.0 and 5.0 kmol m^{-3}. The flow rate of the solution in the cell at the level of the leading edge of the working electrode, v_0, was adjusted at fixed values between 0.1 and 0.7 m s^{-1}. The influence of the pH on the current density distribution was studied at a pH between 9 and 12. Furthermore, the effect of the $Na_2Cr_2O_7$ concentration from 0 to 0.015 kmol m^{-3} was examined.

3. Results

A characteristic result for the current distribution is shown in Fig. 3. In this figure the results for three single measurements, carried out successively within 2 min, are shown by plotting the segment current, I_s, versus the segment number, n_s, from the leading edge of the segmented electrode. Segment number 20 indicates the top segment. The I_s/n_s relation is most accurately fitted by a linear equation. The deviation of the experimental points from the straight line can be assigned to systematic and/or incidental errors. Systematic errors arise because of slight differences in the potentials of the electrode segments and in the geometry of the electrode segments. Fluctuations in the gas bubble/liquid mixture cause incidental errors. These are minimized by repeating the measurement of the current distribution several times and subsequently calculating the average current density distribution. From the I_s/n_s straight line the current density at the top, j_t, and at the leading edge of the working electrode, j_b, were determined by linear extrapolation. From these values the current distributon factor, $B = (j_b - j_t)/j_{av}$, was calculated.

The factor B is used to show the effect of several parameters on the electrode current distribution, such as time of electrolysis, average current density, flow rate of solution, temperature, sodium chloride concentration, sodium dichromate concentration, inter-electrode gap and pH.

First the effect of time of electrolysis on the current distribution factor was investigated. After half an hour of electrolysis of a 1.5 M NaCl solution at 20 A, the current distribution factor B was determined as a function of the current density at decreasing current density. The result is given by curve 1 in Fig. 4. Thereafter, the electrolysis was continued with 20 A for 45 min and subsequently the current distribution factor was again determined as a function of the current density. Curve 2 in Fig. 4 shows the results. The electrolysis with 20 A for 45 min and the measurements of the current distribution factor were repeated. The results are given by curve 3 in Fig. 4. This figure indicates that B/j_{av} curves are straight and parallel to each other and that B decreases with increasing time of electrolysis.

Hypochlorite is formed during the elecrolysis. It has been found that the concentration of hypochlorite is 41, 71 and 90 mol m^{-3} in 4 l of solution after, respectively, the first, the second and the third period of electrolysis with 20 A. The decrease in concentration of NaCl can be neglected and the pH remained at 9 during the series of experiments. It is likely that the decrease in B with increasing time of electrolysis is caused by an increase in the rate of hypochlorite reduction leading to a decrease in the rate of the hydrogen evolution.

Table 1.

Electrode combination		B_0
Segmented electrode	*One-plate electrode*	
Ti/RuO_2–TiO_2 anode	Ti cathode	0.473
Ti/RuO_2 anode	Ti/Pt–Ir cathode	0.440
Stainless steel cathode	Ti/Pt–Ir anode	0.467

Since it is likely that in the absence of hypochlorite, the B/j_{av} curve passes through the origin of the B/j_{av} plane, the current distribution factor at the beginning of the electrolysis, B_0, is given by $B_0 = a_1 \times j_{av}$ where a_1 is the slope of the B/j_{av} curve and does not depend on the time of electrolysis (Fig. 4).

Similar results have been obtained for other electrode combinations. Table 1 shows B_0 for three different electrode combinations at a current density of $6\,kA\,m^{-2}$, a solution flow rate v_0 of $0.3\,m\,s^{-1}$, a sodium chloride concentration of $1.5\,kmol\,m^{-3}$, a temperature of 343 K and an interelectrode gap of 2 mm.

The effect of the solution flow rate, v_0, on the current distribution in the cell is illustrated for a segmented Ti/RuO_2–TiO_2 anode and a one-plate titanium cathode in Fig. 5. Also here, the current distribution factor was determined after various periods of electrolysis. These experiments were carried out in a similar manner to experiments of Fig. 4. Figure 5 shows the curves after the first, the second and the third period of electrolysis with 20 A. From this figure it follows that the current density distribution becomes more uniform with increasing flow rate of solution and with increasing time of electrolysis.

The influence of the interelectrode gap, d_{wt}, on the current distribution factor, B_0, is show in Fig. 6 for a segmented Ti/RuO_2–TiO_2 and a one-plate titanium cathode at different current densities. This figure shows that B_0 decreases with increasing interelectrode gap.

In Fig. 7 the effect of the temperature on the current distribution factor, B_0, is compared for various average current densities for a segmented Ti/RuO_2–

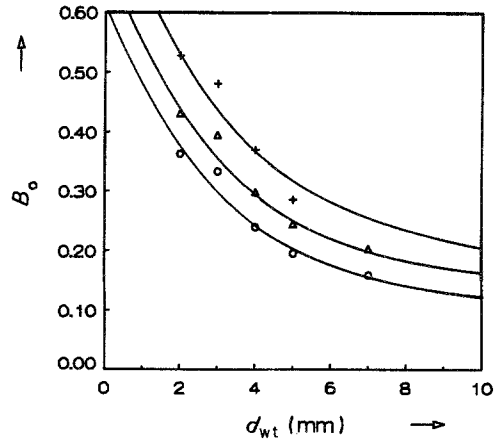

Fig. 6. Dependence of B_0 on the distance between anode and cathode at different current densities. (+) $3.5\,kA\,m^{-2}$; (△) $4.5\,kA\,m^{-2}$; and (○) $6\,kA\,m^{-2}$. Experimental conditions with the exception of the interelectrode gap, d_{wt}, and the average current density: see Fig. 3.

TiO_2 anode with a one-plate titanium cathode. From this figure it follows that B_0 increases with increasing temperature. Similar results have been obtained for the other electrode combinations.

To study the effect of the sodium chloride concentration on B the following experiment was carried out: a solution containing $1.0\,kmol\,m^{-3}$ NaCl was electrolysed for 150 min at 20 A. Subsequently, every minute the current distribution factor was determined at a current density of $5.25\,kA\,m^{-2}$ and a solution flow rate of $0.3\,m\,s^{-1}$ for a period of 10 min. The current distribution factor was constant during this period. Thereafter the NaCl concentration was increased to $1.5\,kmol\,m^{-3}$ by adding an equivalent amount of salt to the solution. Due to the lower resistivity of the solution the average current density increased, and the current density was again adjusted to $5.25\,kA\,m^{-2}$. After periods of half an hour the procedure of addition of NaCl and adjustment of current was repeated. In Fig. 8 the current distribution factor obtained by this procedure is plotted versus the NaCl concentration at a current density of $5.25\,kA\,m^{-2}$ and a solution flow rate of $0.3\,m\,s^{-1}$. The plot illustrates that the current distribution over the anode becomes more uniform with increasing NaCl concentration. In Fig. 8 the resistance of the solution is also given as a

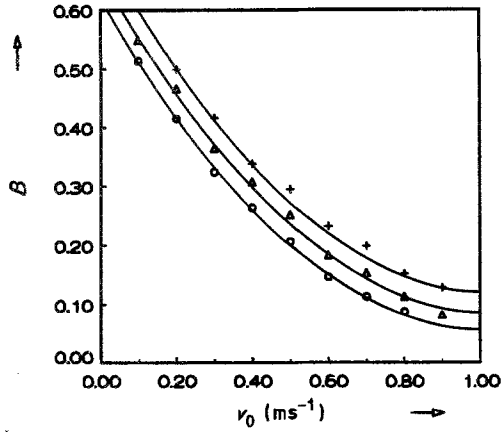

Fig. 5. Effect of the solution flow rate, v_0, on the current distribution factor B at different times of electrolysis. Experimental conditions: see Fig. 4. (+) Curve 1, t_e = 30 min; (△) curve 2, t_e = 75 min; (○) curve 3, t_e = 120 min.

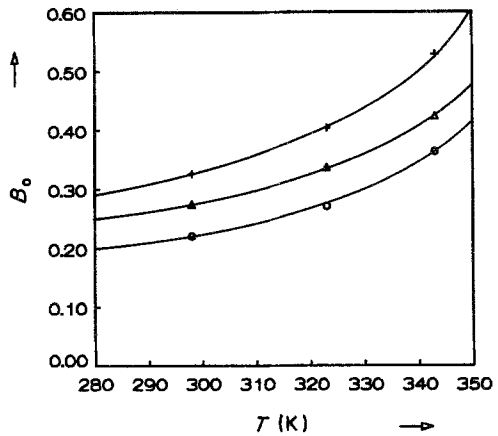

Fig. 7. B_0 vs T curves for different average current densities. (+) $5.0\,kA\,m^{-2}$; (△) $4.5\,kA\,m^{-2}$; (○) $4.0\,kA\,m^{-2}$. For the other experimental conditions see Fig. 3.

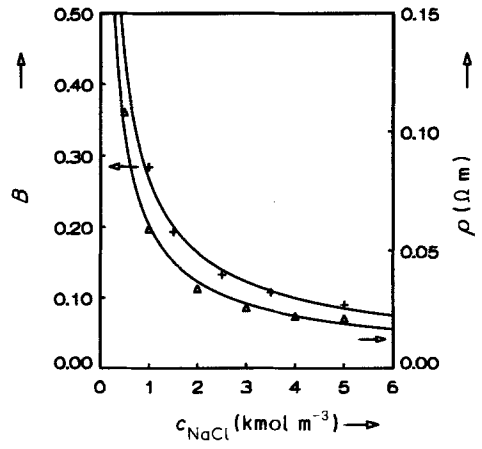

Fig. 8. Effect of the NaCl concentration on the current distribution factor (+) and on the resistivity of solution (△) for an electrolysis with a segmented Ti/RuO_2–TiO_2 anode and a one-plate titanium cathode at j_{av} = 5.0 kA m^{-2}, v_0 = 0.3 m s^{-1}, T = 343 K, d_{wt} = 2 mm and pH = 9.

function of the NaCl concentration. The shapes of both curves indicate that there is a direct relationship between the solution resistance and the current density distribution.

After the measurements of the concentration dependence of B, the same solution was used to study the effect of the pH on the current distribution factor. Again the current distribution factor was measured every minute. After periods of half an hour the pH was successively increased from pH 9 to pH 12. No change in B was observed during the periods where the pH was constant. The results are shown in Fig. 9. This figure indicates that the current distribution factor increases slightly with decreasing pH. Consequently, the current density distribution becomes more uniform with increasing pH.

Figure 10 shows the effect of the two successive additions of the same amount of $Na_2Cr_2O_7$ to the NaCl solution on the current distribution factor B and on the average current density at a solution flow rate of 0.3 m s^{-1}, a temperature of 343 K, an inter-electrode gap of 2 mm, a pH of 9 and an NaCl concentration of 5.0 kmol m^{-3}. $Na_2Cr_2O_7$ concentrations of 7.5 mol m^{-3} were reached after the first and second addition, respectively.

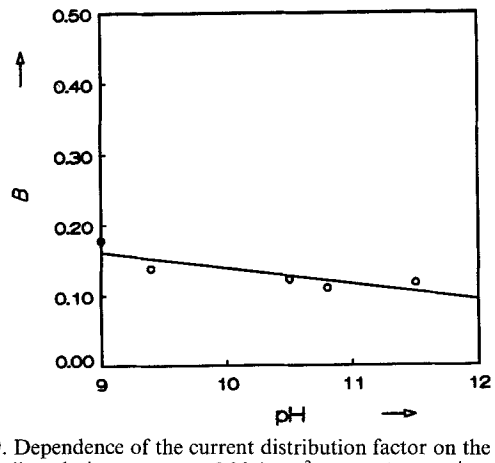

Fig. 9. Dependence of the current distribution factor on the pH of the bulk solution at j_{av} = 5.0 kA m^{-2}, v_0 = 0.3 m s^{-1}, c_{NaCl} = 5.0 kmol m^{-3}, T = 343 K and d_{wt} = 2 mm for experiments with a segmented Ti/RuO_2–TiO_2 anode and a one-plate titanium cathode.

The data points shown in Fig. 10 are due to a single measurement of the current distribution and are plotted versus the time of electrolysis. Before the first addition the average current density and the current distribution factor were constant at 5.25 kA m^{-2} and 0.21, respectively. Directly after the first addition, the average current density decreased strongly and the current distribution factor first rose strongly and thereafter decreased to a value greater than that before the addition. The cell voltage before and during 15 min after the first addition was 3.35 V. Fifteen minutes after the first addition the average current density was adjusted to the same value as before the first addition, and the cell voltage rose to 3.57 V and the current distribution factor, B, increased to 0.43. A further slight increase in B to 0.45 was observed after the second addition of $Na_2Cr_2O_7$. The current distribution remained constant at the same value after the second addition. Consequently, only the first addition of $Na_2Cr_2O_7$ increased the non-uniformity of the current distribution.

4. Discussion

The current density distribution in hypochlorite electrolysis is mainly influenced by the presence of gas bubbles. The evolution of oxygen gas can be neglected because the gas volume of oxygen hardly exceeds 5% of the total gas volume at the applied conditions [8]. Chlorine formed at the anode is transported both as bubbles and in dissolved form to the bulk solution. The efficiency of bubble evolution at an anode in an acidic chloride solution saturated with chlorine at a pressure of 1 atm is rather low. *viz.* about 0.4 for a small platinum anode at j = 6 kA m^{-2}, v_0 = 0.05 m s^{-1} and at 298 K [9]. Taking into account this result, the small chlorine concentration in the solution at the entrance of the cell and the high rate of chlorine hydrolysis due to the high pH of the solution, *viz.* from 9 to 12, it is likely that almost no chlorine is present in the form of gas bubbles. Consequently, the bubbles in the bulk of the solution can be considered as hydrogen bubbles.

Both electrodes, the anode as well as the cathode, are covered by a layer of adhered gas bubbles; the cathode by hydrogen bubbles and the anode by oxygen–chlorine bubbles [10, 11].

It has been found that the concentration of hypochlorite increases at a decreasing rate with time of electrolysis. This is mainly caused by the reduction of hypochlorite at the cathode and the conversion of hypochlorite to chlorate at high temperatures and pH < 10 [12, 13]. Since, for a platinum electrode, the reduction is determined by diffusion at potentials even higher than the reversible hydrogen potential [4], it is likely that this is also the case for the cathodes used in this investigation, *viz.* Ti, Ti/Pt–Ir and stainless steel, at the current density range from 2 to 7 kA m^{-2} where the potential is much more negative than the reversible potential.

From Figs 5 and 6 it follows that the current

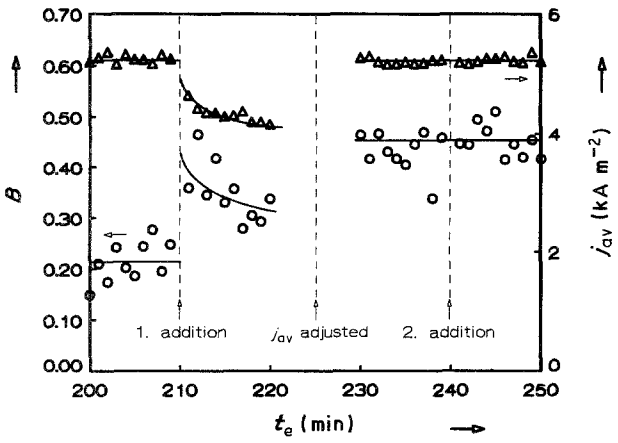

Fig. 10. Effect of two subsequent additions of sodium dichromate to the NaCl solution on the current distribution factor and on the average current density for an NaCl electrolysis with a segmented Ti/RuO_2–TiO_2 anode and a one-plate titanium cathode at $v_0 = 0.3\,m\,s^{-1}$, $T = 343\,K$, $d_{wt} = 2\,mm$, $c_{NaCl} = 1.5\,kmol\,m^{-3}$ and pH 9. Sodium dichromate concentration: $7.5\,mol\,m^{-3}$ after the first addition and $15.0\,mol\,m^{-3}$ after the second. The cell voltage before and directly after the first addition is 3.35 V, and that before and directly after the second addition is 3.57 V. The values of B are determined by a single measurement after each minute.

distribution factor becomes smaller with increasing time of electrolysis and, so, with increasing concentration of hypochlorite. An increase in the rate of hypochlorite reduction means a decrease in the rate of hydrogen evolution. Consequently, the gas void fraction in the cell decreases with increasing rate of hypochlorite reduction.

An estimate of the limiting current density of the hypochlorite reduction can be calculated. The average thickness of the Nernst diffusion layer, δ for a 50-cm-long electrode is about $0.8 \times 10^{-5}\,m$ at $v_0 = 0.3\,m\,s^{-1}$ and 298 K [13]. Using the diffusion coefficient of hypochlorite $D = 1.10 \times 10^{-9}\,m^2\,s^{-1}$ [14] it can be calculated that the limiting diffusion current is $1.10\,kA\,m^{-2}$ at a hypochlorite concentration of $41\,mol\,m^{-3}$. This value of the limiting current and the intersect of curve 1 with the j_{av} axis in Fig. 5 are of the same order of magnitude. Consequently, the reduction of hypochlorite significantly affects the current distribution over the electrodes.

This conclusion is supported by the effect of sodium dichromate addition on the current distribution factor (Fig. 10). It is well known [5] that a chromium oxide layer is formed on the cathode during hypochlorite electrolysis in the presence of dichromate. This diaphragm-like layer diminishes the transfer of hypochlorite to the cathode and so the reduction of hypochlorite [6]. The current drop after the first addition of sodium dichromate, shown in Fig. 10, is caused by the diminishing hypochlorite reduction and by the extra resistance of the chromium oxide layer formed on the cathode.

Since the intersection point of the B/j_{av} curve with the j_{av} axis is closely related to the hypochlorite concentration, it is likely that the current distribution factor, B, is given by $B = a_1 j_{av,H}$ where $j_{av,H}$ is the average current density used for hydrogen evolution. From Table 1 it can be concluded that the current distribution over both electrodes – anode and cathode – is practically the same. The different nature of the electrode material does not significantly affect the current distribution in the cell.

The current distribution becomes more uniform with increasing flow rate of solution (Fig. 5), distance between both electrodes (Fig. 6) and concentration of sodium chloride (Fig. 8) and with decreasing temperature (Fig. 7).

The current distribution depends on the kinetics of the electrode reactions and on the ohmic resistance of the solution between the electrodes. The latter factor depends on the gas void fraction and its distribution over the gap between both electrodes. In the most simple model the gas void fraction in the cell is constant over the gap between both electrodes. According to the Bruggemann equation, the solution resistance R_s is given by [16]

$$R_s = \varrho(1 - \varepsilon)^{-3/2} d_{wt} \qquad (9)$$

where ε is the gas void fraction, ϱ is the resistivity of solution and d_{wt} is the interelectrode gap. The cell potential is the sum of the reversible cell potential, U_0, the overpotential at the anode, $\eta_a = b_a \log |j|/j_0$, and the cathode, $\eta_c = b_c \log |j|/j_0$ and the ohmic potential drop over the solution, jR_s

$$U = U_0 + (b_a + b_c) \log |j|/j_0 + jR_s \qquad (10)$$

where U_0 is the reversible cell potential, b_a and b_c are the anodic and cathodic Tafel constants, respectively, j is the current density, j_0 is the exchange current density and R_s is the surface area resistance of solution.

Assuming that the cell potential is constant over the height of the electrode, the difference between the current density at the bottom and at the top can be calculated

$$(b_a + b_c) \log \frac{j_b}{j_t} = j_t R_{s,t} - j_b R_{s,b} \qquad (11)$$

where the subscripts b and t indicate the bottom and the top of the electrode, respectively.

Since

$$B = (j_b - j_t)/j_{av} \qquad (12)$$

it can be shown that

$$(b_a + b_c) \log \frac{(1 + 0.5B)}{(1 - 0.5B)} = j_{av} R_{s,t}(1 - 0.5B) - R_{s,b}(1 + 0.5B) \qquad (13)$$

When no hypochlorite reduction occurs, the current distribution factor is given by $B = B_0$. Using Equations 9 and 13, B_0 can be calculated at various temperatures. It has been found that the sum of the Tafel slopes is independent of the temperature and is 0.45 V for a Ti/RuO_2–TiO_2 anode combined with a Ti cathode. The resistivity of a solution of $1.5\,kmol\,m^{-3}$ NaCl at various temperatures is given in Fig. 11 [17]. Taking into account the temperature effect on the molar gas volume and on the water vapour pressure, B_0 has been calculated at various temperatures for a

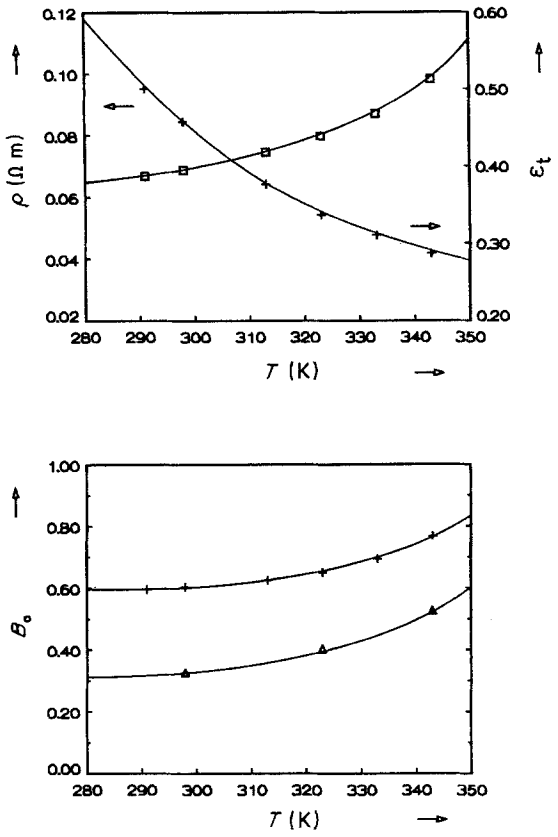

Fig. 11. The effect of the temperature on the resistivity, ϱ, on the gas void fraction at the top of the electrode, ε_t, and on the experimental and the theoretical B_0 at a current density of $6\,kA\,m^{-2}$, a flow velocity of $0.3\,m\,s^{-1}$, an interelectrode gap of 2 mm, and an NaCl concentration of $1.5\,kmol\,m^{-3}$. ($\triangle$) experimental; and (+) theoretical values of B_0.

solution flow velocity of $0.3\,m\,s^{-1}$, an interelectrode gap of 2 mm, an average current density of $6\,kA\,m^{-2}$ and an NaCl concentration of $1.5\,kmol\,m^{-3}$. A comparison of the calculated and experimental values of the current density distribution as a function of the solution temperature is given in Fig. 11. From this figure it can be concluded that the current distribution factor, B_0, increases with increasing temperature for both experimental and theoretical values of B_0 and that the calculated values of B_0 are much higher than the experimental one. The temperature clearly affects two factors which have an opposite effect on the resistance of the solution. On the one hand the resistivity of the bubble free solution decreases and on the other hand the gas void fraction increases (Fig. 11). The current distribution becomes more uniform with decreasing resistivity of the solution (Fig. 8). Consequently, because B_0 increases with increasing temperature, the effect of the temperature on the gas void fraction is greater than on the resistivity of the solution.

From the great difference in the theoretical and the experimental values of B_0, shown in Fig. 11, it follows that the simple model for the horizontal distribution of the gas void fraction is not useful for a hypochlorite electrolysis cell. Consequently, the bubble layers adjacent to the electrodes have to be taken into account. A new model is under investigation.

References

[1] N. Ibl and H. Vogt, in 'Comprehensive Treatise of Electrochemistry', Plenum Press, New York (1981) Vol. 2, p. 173 ff.
[2] N. Ibl and D. Landolt, *Electrochim Acta* **15** (1970) 1165.
[3] O. Schwarzer and R. Landsberg, *J. Electroanal. Chem.* **19** (1968) 405.
[4] J. A. Harrison and Z. A. Khan, *J. Electroanal. Chem.* **30** (1971) 87.
[5] E. Mueller, *Z. Electrochem* **5** (1899) 469.
[6] F. Förster, Elektrochemie wässriger Lösungen, J. Ambrosius Barth, Leipzig (1923) 598.
[7] B. B. E. Bongenaar-Schlenter, Thesis, Eindhoven (1985).
[8] J. M. Alice, B. K. Sadanada Rao and G. Venkatamoran, *Indian. Chem. Eng.* **28** (1986) 49.
[9] J. M. Chin Kwie Joe, L. J. J. Janssen, S. J. van Stralen, J. H. G. Verbunt and W. H. Sluyter, *Electrochim Acta* **33** (1988) 769.
[10] H. Vogt, *Electrochim. Acta* **28** (1983) 314.
[11] C. W. M. P. Sillen, Thesis, Eindhoven (1983).
[12] G. R. Heal, A. T. Kuhn and R. B. Lartey, *J. Electrochem. Soc.* **124** (1977) 1690.
[13] L. J. J. Janssen and E. Barendrecht, in 'Modern Chlor-Alkali Technology' (edited by K. Wall), Chichester (1986) Vol. 3, p. 430.
[14] H. M. Gijsbers and L. J. J. Janssen, to be published.
[15] L. Czarnetzki and L. J. J. Janssen, *Electrochim. Acta* **33** (1988) 561.
[16] R. E. de la Rue and C. W. Tobias, *J. Electrochem. Soc.* **106** (1959) 827.
[17] E. W. Washburn (editor), 'International Critical Tables', McGraw-Hill, New York (1929).